

# Universal Substructure Distributions in $\Lambda$ CDM halos: Can we find a Fossil Group?

Elena D’Onghia<sup>1</sup>  $\star$ , Andrea V. Macciò<sup>1,2</sup>, George Lake<sup>1</sup>, Joachim Stadel<sup>1</sup>, Ben Moore<sup>1</sup>

<sup>1</sup>*Institute for Theoretical Physics, University of Zürich, Winterthurerstrasse 190, CH-8057 Zürich, Switzerland*

<sup>2</sup>*Max-Planck-Institute for Astronomy, Königstuhl 17, D-69117 Heidelberg, Germany*

submitted to MNRAS

## ABSTRACT

We use large cosmological N-body simulations to study the subhalo population in galaxy group sized halos. In particular, we look for fossil group candidates with typical masses  $\sim 10$ -25% of Virgo cluster but with an order of magnitude less substructure. We examine recent claims that the earliest systems to form are deficient enough in substructure to explain the luminosity function found in fossil groups. Although our simulations show a correlation between the halo formation time and the number of subhalos, the maximum suppression of subhalos is a factor of 2-2.5, whereas a factor of 6 is required to match fossil groups and galaxies. While the number of subhalos depends weakly on the formation time, the slope of the halo substructure velocity function does not. The satellite population within Cold Dark Matter (CDM) halos is self-similar at scales between galaxies and galaxy clusters regardless of mass, whereas current observations show a break in self-similarity at a mass scale corresponding to group of galaxies.

**Key words:** galaxies: formation – galaxies: halos – galaxies: structure – cosmology: theory – dark matter – large-scale structure of Universe – methods: numerical, N-body simulation

## 1 INTRODUCTION

In the current paradigm for cosmological structure formation, dark halos collapse from initial gaussian density fluctuations and grow by accretion and merging in a hierarchical fashion. A longstanding prediction of the theory is that the subhalo (or satellite) population is self-similar, meaning simply that low mass systems, such as galaxies are scale-down versions of larger systems, like galaxy clusters. A galaxy such as the Milky Way is predicted to have nearly the same scaled distribution of substructures as a more massive galaxy cluster such as Virgo (Moore et al. 1999, Klypin et al. 1999). This prediction is tested by using the substructure velocity distribution function that expresses the number of sub-halos with circular rotational velocity  $V_{circ}$  greater than a certain fraction of the circular velocity of the parent halo  $V_{par}$ .

Cosmological numerical simulations confirm the expectations predicting about 500 satellites with  $V_{circ}/V_{par} > 0.05$  within 500 kpc of the Milky Way. Accounting for the most recent discoveries of SLOAN data for fainter galaxies (i.e. Willman et al. 2005, Kleya et al. 2005) up to date less than 30 satellite galaxies have been observed in the Lo-

cal Group including underluminous systems that likely have even lower  $V_{circ}/V_{par}$  pointing out a missing satellite problem in the current paradigm for structure formation. Proposed solutions to this puzzle invoke the reionization of the universe at high redshift combined with the local injection of energy from star formation (Bullock et al. 2000, Somerville 2002, Benson et al. 2002). These mechanisms may be invoked to suppress galaxy formation in halos below  $30 \text{ km s}^{-1}$  reconciling the predictions with observations in the Local Group. Recently, however, D’Onghia & Lake (2004) have shown that fossil groups with intermediate mass between the Local group and the Virgo cluster are systems with paucity of substructures pointing to a missing galaxy problem in higher mass systems.

In fossil groups, a giant E or cD galaxy dominates with the next brightest group member being at least 2 R-band magnitudes fainter. The archetype is RXJ1340.6+4018, an isolated, bright ( $M_R = -22.7$ ) elliptical galaxy at  $z=0.171$ , surrounded by a halo of hot gas and dark matter (Jones et al. 2000). Its total mass is  $\sim 25\%$  of the Virgo cluster.

With  $V_{par} \sim 60\%$  of Virgo, the escape energies of their missing substructures in the fossil group are  $\sim 10$  times larger than the satellites missing from the Local Group, far

$\star$  Marie Curie Fellow; elena@physik.unizh.ch

too large to be explained by proposed suppression mechanisms.

Subsequent observations have shown that fossil groups are clearly virialized objects in which a central galaxy is embedded in a X-ray halo with a luminosity 10–60 Hickson Groups, many of which show only a faint X-ray emission and may be either evolving systems (Miles et al. 2004) or fake associations; they are more useful than loose groups, which are often unvirialized structures contaminated by sighting down filaments (Hernquist et al. 1995).

Recently, however, Kravtsov et al. (2004) proposed that luminous dwarf spheroidals in the Local Group descend from downsizing of relatively massive ( $> 10^9 M_\odot$ ) high- $z$  systems by processes such as tidal stripping. Again, this idea may help explaining the lack of substructures in the Local Group (Mayer et al. 2007) but it is unlikely to explain how massive objects ( $\sim 10^{10} - 10^{11} M_\odot$ ) survive in a Virgo-size object where the ram stripping is more efficient and yet are absent in fossil groups of nearly the same mass.

Is RXJ1340.6+4018 representative of the whole class of fossil groups? Early work on the fossil groups focused on the magnitude gap in the luminosity function and suggested that it owed to early formation times and subsequent merging (Jones et al. 2003, D’Onghia et al. 2005). However, little work has been devoted to understand the truly remarkable feature that nearly every group with a magnitude gap of 2 has a substructure function like the Local Group. The known exceptions are RX J1552.2+2013 (e.g. Cypriano, Mendes de Oliveira and Sodr e 2006) and a cluster of galaxies discovered recently (Gastaldello et al. 2007) which are rich enough with substructure that they have been called ”fossil clusters”.

The self-similarity of the subhalo population resulting from cosmological N-body simulations is still debated (e.g. De Lucia et al. 2004, Diemand et al. 2007). In this context, Zentner et al. (2005) used semi-analytical models to claim that early formation times lead to significantly less substructure providing a natural explanation of the lack of galaxies in fossil groups.

These are the issues that we address in this paper. We present N-body simulations of galaxy group halos to clarify the cosmic abundance and variance of substructure as related to magnitude gaps and formation history. The plan of the paper is as follows. In §2 we present details of the numerical simulations and analysis procedure. §3 presents the results, whilst 4 summarizes our conclusions.

## 2 NUMERICAL METHODS

### 2.1 Simulations

We analyze two  $\Lambda$ CDM simulations with cosmological parameters taken from the best-fits for WMAP1 (Spergel et al. 2003) and WMAP3 (Spergel et al. 2006). These have present-day matter density parameters  $\Omega_m=0.268$  ( $0.238$  for WMAP3); cosmological constants contribution  $\Omega_\Lambda=0.732$  ( $0.762$ ); baryonic contributions  $\Omega_b, h=0.044$  ( $0.042$ ); and Hubble parameters  $h = 0.71$  ( $0.73$ ) ( $H_0 = 100 h$  km s $^{-1}$  Mpc $^{-1}$ ). The mass fluctuation spectrum has a spectral index  $n = 1$  ( $0.951$ ), and is normalized by the linear rms fluctuation on 8h $^{-1}$ Mpc,  $\sigma_8 = 0.9$  ( $0.75$ ). The initial conditions are generated with GRAFIC2 (Bertschinger 2001).

All runs started at redshifts sufficiently high to ensure that the absolute maximum density contrast is still in the linear regime.

We followed the evolution of  $600^3$  particles with masses of  $8.98 \times 10^7 h^{-1} M_\odot$  and  $8.67 \times 10^7 h^{-1} M_\odot$  for WMAP1 and WMAP3 in a box 90 Mpc (comoving) on a side using the treecode PKDGRAV (Stadel 2001). Gravitational interactions between pairs of particles are softened in comoving coordinates with a spline softening length  $\epsilon = 1.16$  kpc; forces are completely Newtonian at twice this distance. The particles have individual timesteps  $\Delta t_i = 0.2 \sqrt{\epsilon/a_i}$  where  $a$  is particle’s acceleration. The node-opening angle is  $\theta = 0.7$  after  $z = 2$  and  $\theta = 0.55$  earlier to provide higher force accuracy when the density is nearly uniform. Cell moments are expanded to fourth order.

### 2.2 Halo identification

Bound structures with a minimum of 250 particles at  $z=0$  are identified using the Spherical Overdensity (SO) algorithm (Macci o et al. 2007) with a linking length  $l$  equal to 0.2 times the mean interparticle separation. For each halo, we fix the center at the most bound particle and find the mass within the virial radius where the spherical overdensity relative to the critical density for closure is  $\Delta(z=0) \simeq 96.7$  and  $\Delta(z=0) \simeq 93.5$  for WMAP1 and WMAP3 respectively (Mainini et al. 2003). We discard structures with less than 250 particles and iterate the procedure to convergence. If a particle is a potential member of two groups, it is assigned to the most massive one.

We select for our analysis all halos with masses in the range  $M = 1.75 - 5.25 \times 10^{13} M_\odot$ , resulting in 28 galaxy group sized halos for WMAP1 and 16 groups for WMAP3 with  $N_{vir}$  between 200,000 and 600,000 particles.

### 2.3 Subhalo Identification

The subhalo population is identified with SKID (Stadel 2001), which calculates local densities using an SPH kernel, then moves particles along the density gradient until they oscillate around a point characterized by some length  $l$ . Then particles are linked together using the friend-of-friend algorithm with a linking length equal to  $l$ . Using a linking length 4 times the gravitational softening SKID algorithm identifies the subhalo population inside each halo. Unfortunately by assuming this linking length the parent halo mass may be underestimated. On the other hand using a larger linking length, 10 times the gravitational softening can cure this problem, but then some of the small Sybilla’s are missed. Therefore we used a combination of the subhalo catalogs obtained with these two linking lengths in order to create the complete catalog of subhalos and to calculate their correct structural parameters. We select for our analysis only subhalos with  $M > 4.5 \times 10^9 h^{-1} M_\odot$ .

### 2.4 Halo formation redshift

The assembly history of each halo may be studied using halo catalogs constructed at various times during the evolution of the system. For the purposes of our analysis, we concentrate on the period  $0 < z < 3$ . Halos identified at  $z > 0$  are

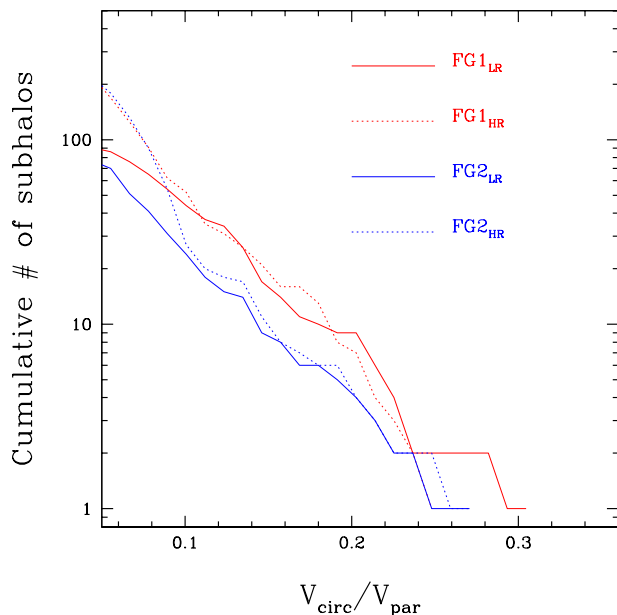


**Figure 1.** Cumulative subhalo velocity distribution function by different resolutions for two halos of the sample. Solid lines correspond to the lower resolution run and dotted lines to the high resolution run of the same halo.

said to be *progenitors* of a  $z = 0$  system if at least 50% of its particles are found within the virial radius of the latter. Using this definition we can identify, at all times, the list of progenitors of a given  $z = 0$  galaxy group sized halo and track their properties through time. For each halo, we use its mass assembly history (MAH) to determine its formation time. The MAH is defined using the most massive progenitor and is usually well-fit by:

$$M(z) = M_0 \exp \left[ \frac{-2z}{(1+z_f)} \right], \quad (1)$$

with  $z$  the redshift,  $M_0$  the halo mass at present day and  $z_f$  the formation redshift, defined as the redshift at which the fitted halo MAH slope assumes the value of 2 (Wechsler et al. 2002).

## 2.5 Numerical Resolution Test

Only subhalos significantly larger than the gravitational softening survive the tidal forces of the parent halo. To test the scale where this is significant, we re-simulated two galaxy group sized halos from the WMAP1 simulation with 8 times higher mass resolution. The test halos have 3,000,000 particles within the virial radius at  $z=0$ . Figure 1 shows that the low resolution (solid lines) and the high resolution runs (dotted lines) are in fairly good agreement for subhalos above our adopted resolution limit of  $V_{\text{circ}}/V_{\text{par}} = 0.1$ .

## 2.6 Fossil group sample selection criterion

We aim to select fossil groups in our sample of galaxy group sized halos. Ideally we want to determine a distribution of

magnitude gaps and its relationship to the subhalo population in our sample. Since luminosity and magnitudes are not defined in our simulations, the identification of a magnitude gap between the first and second brightest member must be translated to a circular velocity gap. If the Faber-Jackson (1976) relationship holds, then a 2 magnitude gap in the luminosity function corresponds to a circular velocity ratio  $V_{\text{circ}}^{2\text{nd}}/V_{\text{circ}}^{1\text{st}} \sim 0.6$ , while a gap of 2.5 magnitudes would be  $V_{\text{circ}}^{2\text{nd}}/V_{\text{circ}}^{1\text{st}} \sim 0.55$ . In observed systems, the brightest halo lies at the center of the X-ray emission as well as at the centroid of the redshift distribution, but its velocity dispersion is significantly less than the overall dispersion of the group, or equivalently, its X-ray temperature. The first brightest galaxy in our simulations is subsumed into the parent halo, so we need to calculate the ratio of  $V_{\text{circ}}^{2\text{nd}}/V_{\text{par}}$  that characterizes a fossil group. In the case of RXJ1340.6+4018, its luminosity function has a magnitude gap of 2.5, corresponding to the ratio of  $V_{\text{circ}}^{2\text{nd}}/V_{\text{circ}}^{1\text{st}} = 0.55$  and  $V_{\text{circ}}^{1\text{st}}/V_{\text{par}} \sim 0.65$ , so that  $V_{\text{circ}}^{2\text{nd}}/V_{\text{par}} \sim 0.35$ . We adopt  $V_{\text{circ}}^{2\text{nd}}/V_{\text{par}} < 0.35$  as a conservative criterion for a group with an appropriate magnitude gap. We note that the Local Group and Centaurus A group also meet this criterion and have substructure functions comparable to RXJ1340.6+4018. Subhalo mass determination in collisionless N-body simulations is uncertain. When dissipation is included in simulations, the subhalos number increases because the substructures become more robust and can survive to the very center of the parent halos (Nagai & Kravtsov 2005, Macciò et al. 2006a). Hence we measured the circular velocities of substructure at the time of *infall* into the larger halos (see also Strigari et al. 2007). After the subhalo falls into the parent halo it loses mass and its circular velocity decreases over time. Henceforth we compare the subhalo circular velocity at infall time with the observational data, not the subhalo circular velocities measured at present time.

Figure 2 shows the circular velocity of the second most massive subhalo compared to that of the parent halo for our simulated groups. The groups with  $V_{\text{circ}}^{2\text{nd}}/V_{\text{par}} < 0.35$  are selected as candidate fossil groups. Only 18% of groups qualify, in fair agreement with the observed rate (Jones et al. 2003, van den Bosch et al. 2007). But, does their substructure function look like that one of the fossil group RXJ1340.6+4018?

## 3 RESULTS

### 3.1 Substructure function for different cosmological parameters

We define a system to have a *galaxy-like* substructure function when it rescales to that of the Milky Way or equivalently RXJ1340.6+4018 (see e.g. Figure 1 in D’Onghia & Lake 2004). The opposite behavior would be a system with a *cluster-like* behavior, e.g. a rescaled Virgo cluster. The cumulative subhalo velocity distribution function of the halo sample is shown in Figure 3. Note that in this figure we remove the most massive object (i.e. the parent which should include the most massive galaxy) from the cumulative substructure velocity distribution.

The top (bottom) panel is the simulations with WMAP1 (WMAP3) cosmological parameters. The candi-

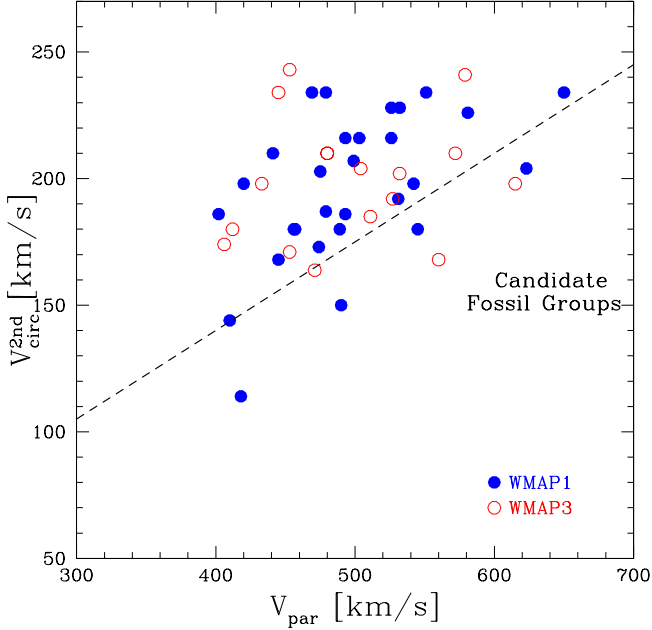


**Figure 2.** The circular velocity of the second most massive subhalo versus the circular velocity of the parent halo in the sample of group sized halos for the two set of simulations with WMAP1 (filled symbols) and WMAP3 (empty symbols) cosmological parameters. The dashed line corresponds to the dividing line for a velocity gap comparable to that observed in fossil groups.

date fossil groups are shown by dashed lines against a background of solid lines for the normal groups. The panels show that the principal difference between the two realizations is that there are fewer group-sized halos with WMAP3 parameters. There is no statistically significant difference between the total number of subhalos with  $V_{circ}/V_{par} > 0.1$  for candidate fossil groups and normal groups in the two realizations. The cumulative substructure velocity distribution functions also show similar trends.

### 3.2 Comparison to observational data

The range of cumulative substructure velocity distribution functions for all the galaxy group sized halos is shown in Figure 4 as compared to the observed ones for galaxy clusters inferred from SDSS data (Desai et al. 2004). The agreement between predictions and observations is encouraging, although the observed cumulative distribution exhibits a broader range for  $V_{circ}^{2nd}/V_{par}$  from 0.25 to 0.8, whereas the second most massive subhalo in the simulations is never larger than 50% of the parent halo. The larger spread might owe to uncertainties in the estimate of the parent’s halo velocity dispersion from a relatively small number of member velocities. The trend of the cumulative subhalo velocity function in simulations agrees well with the one inferred from galaxy clusters. Note that Figure 4 shows that there are galaxy clusters with the second most massive member having  $V_{circ} \sim 25\text{-}30\%$  of the parent halo, showing evidence for magnitude gaps in SDSS data.

Figure 5 shows the range of cumulative subhalo velocity distribution functions for candidate fossil groups in simula-

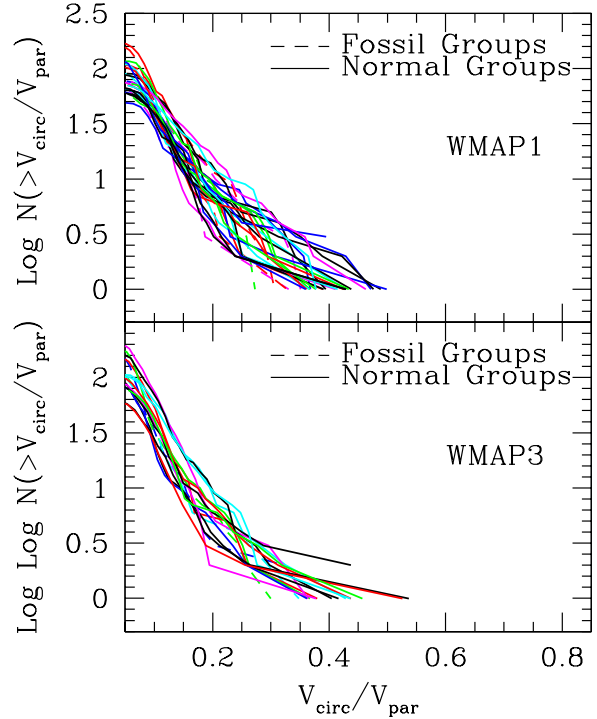


**Figure 3.** Cumulative substructure function for the group sized halos for the different cosmological parameters: WMAP1 in the top panel and WMAP3 in the bottom. Solid lines correspond to normal group sized halos, while dashed lines are the candidate fossil groups.

tions, marked by shaded areas, as compared to the observed ones for RXJ1340.6+4018, the Local Group and Centaurus A (D’Onghia & Lake 2004 for a compilation and reference therein). The Local Group uses data from Mateo et al. (1998), Odenkirchen et al. (2001) and Kleyna et al. (2005); we used the results of Kazantzidis et al. (2004) to convert three-dimensional velocity dispersion into circular velocity. We considered the number of satellites per central galaxy instead of considering the Local Group as a whole. This makes the comparison with simulations straightforward (see Macciò et al. 2006b for more details).

Note that while we find systems with appropriate gaps in velocity between the second most massive subhalo and the most massive one, the cosmic variance in CDM simulations is insufficient to explain the cumulative number of subhalos with circular velocity less than 20% of observed systems (e.g.  $V_{circ}/V_{par} < 0.2$ ).

Numerical simulations performed with WMAP1 and WMAP3 parameters give almost identical results; the narrower region covered by the velocity distribution function in WMAP3 owes to the lower number of candidate fossil groups. These systems populate the lower region of the shaded area shown in Figure 4. The slope of the function agrees well with the one inferred from normal groups and galaxy clusters. Yet, both WMAP1 and WMAP3 models over-predict the total number of substructures relative to

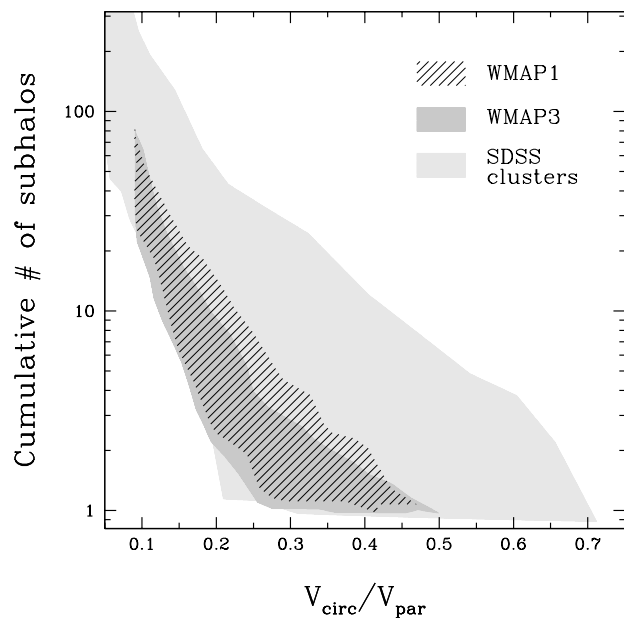


**Figure 4.** Observed cumulative substructure function within galaxy clusters inferred from SDSS data, light gray area (Desai et al. 2004) compared to  $\Lambda$ CDM predictions for all the galaxy group sized halos. The areas represent N-body simulation results for galaxy groups extracted from WMAP1 (diagonal texture) and WMAP3 simulations (gray area). The substructure function is the number of objects with velocities greater than a fraction of the parent halo’s velocity.

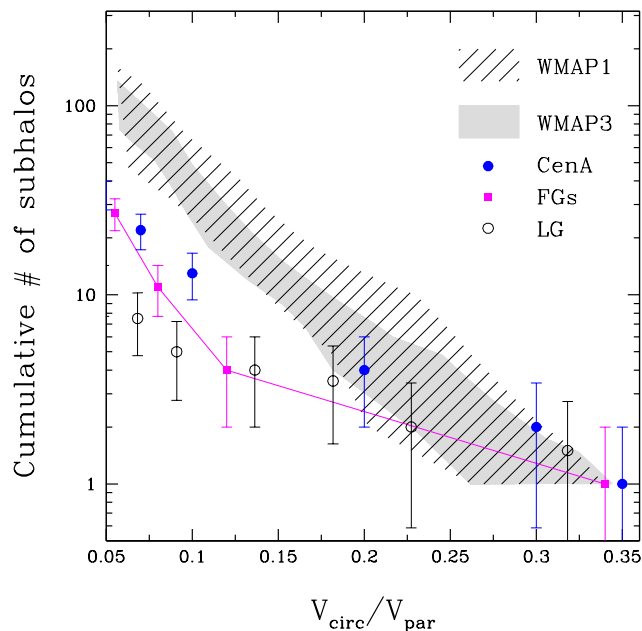


**Figure 5.** Observed cumulative substructure function within RX J1340.6+4018, Virgo cluster, the Local Group and Centaurus A compared to  $\Lambda$ CDM predictions. The shaded area and the represent N-body simulation results for candidate fossil groups extracted from WMAP1 (diagonal texture) and WMAP3 simulations (gray area).

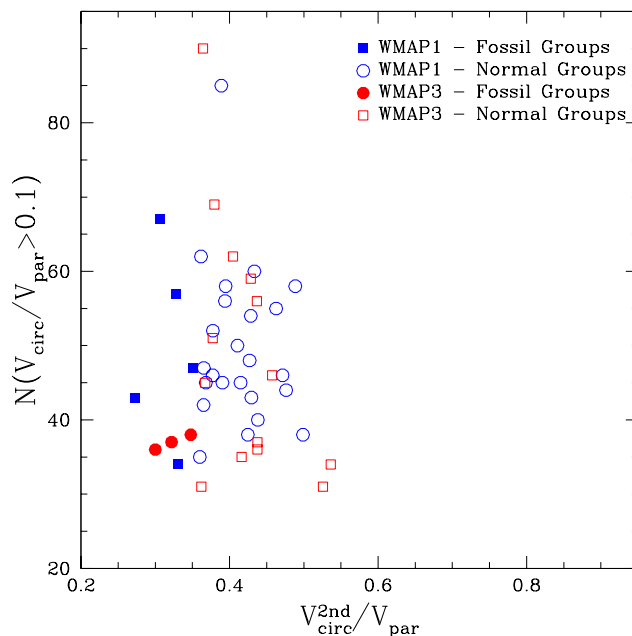


**Figure 6.** Total number of subhalos with circular velocity larger than 10% of the parent circular velocity is plotted against the circular velocity of the second most massive subhalo normalized to the parent halo velocity

Centaurus A and RXJ1340.6+401. Especially for this latter one the discrepancy in the velocity range of subhalos with circular velocity larger than 10% is a factor of six. Can this discrepancy owe to uncertainties in the estimate of the total mass (circular velocity) of the parent halo of RXJ1340.6+401? If the total mass is lower than estimated<sup>†</sup> the points in Figure 5 may shift on the right leading to a fair agreement with the expectations (dashed area). However the X-ray temperature is  $\sim 1$  KeV for the archetype fossil group, meaning a circular velocity of the parent halo at least 580 km/s, so the points can’t be shifted to the right to obtain a better agreement.

Also, dynamical friction and merging are not a general solution to the discrepancy. These dynamical effects are included in the full numerical simulations. Any specific substructure function evolves in the same way by dynamical friction and merging independent of the parent mass (D’Onghia & Lake 2004). Dynamical friction can be important in promoting the merger of the largest objects in less than one Hubble time but dynamical friction alone will not create substructure functions that are different for different parent masses. Clearly galaxies could have had a long time to evolve by dynamical friction, but this is also included in the simulations and does not affect the substructure function below  $V_{circ}/V_{par}$  of 0.2.

Figure 6 shows that the total number of substructures with  $(V_{circ}/V_{par} > 0.1)$  in our simulations is independent of any velocity gap:  $V_{circ}^{2nd}/V_{par}$ . Yet, we don’t find a halo

<sup>†</sup> The velocity dispersion for the system is quoted  $\sigma \sim 380$  km/s with great uncertainties due to the low number of galaxy members (Jones et al. 2000).

population as poor in substructure as RXJ1340.6+4018 and the Local Group.

### 3.3 Substructure abundance and formation redshift

Recently, using semi-analytic models, Zentner et al. (2005) have highlighted the possibility that early forming halos may have significant less substructures, providing a potential explanation of the lack of substructures in the observed fossil groups.

We explore this claim in Figure 7, where the total number of subhalos with circular velocity larger than 10% of the parent halo is shown as a function of the formation redshift ( $z_f$ ) of the parent halo and the two sets of cosmological parameters. Both panels show that there is an anticorrelation between the halo formation redshift and the total number of substructures. Halos that form earlier exhibit a lower number of satellites within a factor two for a cosmology with WMAP1 parameters and slightly larger and with more spread adopting WMAP3 parameters. We tested also the distribution of the halo formation redshift of all the halos selected in the WMAP1 and WMAP3 simulations. Fossil groups and normal groups in the range of mass of  $1 - 5 \times 10^{13} M_\odot$  here adopted tend to form in a narrow range of redshift centered around  $z=1.5$  and  $z=0.9$  for cosmologies with WMAP1 and WMAP3 parameters, respectively. The candidate fossil group halos tend to form slightly earlier than the normal groups ones, even if the sample of fossil groups is limited.

Is this the solution to the missing galaxy question in RXJ1340.6+4018? In Figure 7 we draw three additional horizontal lines tracing the total number of observed galaxies with circular velocity larger than 10% of the parent halo velocity ( $V_{circ}/V_{par} \geq 0.1$ ) for the galaxy group Centaurus A, RXJ1340.6+4018 and the Local Group. While the early formation redshift can reduce on average of a factor two the total number of satellites in simulations, the observations show a discrepancy greater than a factor of five. *We conclude that the early formation time per se can reduce but not reconcile the discrepancy between the observed total number of satellites to the number predicted by numerical simulations in galaxy groups.*

Is the anticorrelation between total number of satellites and redshift formation exhibited in Figure 6 in conflict with the previous finding of self-similarity of the subhalo population of dark matter halos? In order to assess this effect we analyzed separately for each halo the *normalization* of the cumulative velocity distribution function and its slope as a function of the formation redshift. The substructure function of a all halos is known to be approximated by the following power law:

$$N \left( > \frac{V_{circ}}{V_{par}} \right) = V_0 * \left( \frac{V_{circ}}{V_{par}} \right)^\gamma \quad (2)$$

with  $\gamma = -2.75$  over a wide range of mass and cosmological models (Klypin et al. 1999, Klypin et al. 2003). For each halo we fit the power law in the range of  $V_{circ}/V_{par}$  between 0.1 and 0.3 in order to avoid to bias the fossil group candidates in respect to the normal group halos, since the first ones have, by definition a lack of subhalos

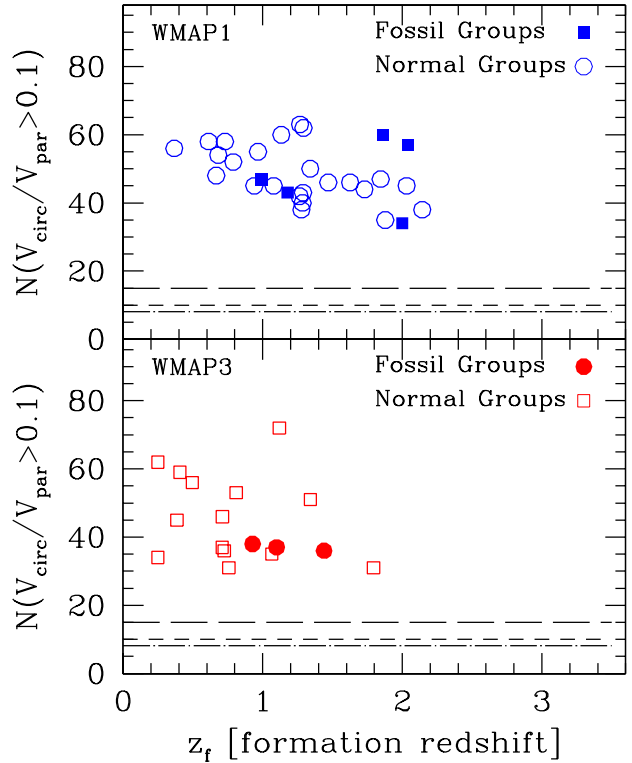


**Figure 7.** Total number of satellites with circular velocity larger than 10% of the parent circular velocity versus the formation redshift of the parent halo. Solid (red) circles mark normal group sized halos, open (blue) squares the candidate fossil group halos. Top and bottom panel show results for the WMAP1 and WMAP3 simulations, respectively. The three lines on the bottom of the plot show observational results inferred for Centaurus A, RXJ1340.6+4018 and the Local Group.

for  $V_{circ}/V_{par} > 0.35$ . During the fitting procedure the normalization  $V_0$  and the slope  $\gamma$  are treated as free parameters. The values and associated uncertainties of  $V_0$  and  $\gamma$  are determined via a  $\chi^2$  minimization procedure using the Lavenberg & Marquart method.

The slope distribution of all the halos selected at  $z=0$  is shown by the histogram in the left panel of Figure 8. The panel on the right of the Figure 8 shows the lack of correlation between the slope  $\gamma$  of the substructure function of each halo and its formation redshift  $z_f$ .

*We conclude that only the normalization of the cumulative velocity distribution function of satellites anticorrelates with the formation time, the slope does not.* This result highlights that non-linear structures in CDM models are self-similar, independent of the formation time and insensitive to the difference in cosmological parameters used in the two simulations. Thus, while the slope of the cumulative substructure function is set by the cosmological model (setting the self similarity of dark halos), its normalization depends on the local environment and on the formation history of the halo.

We draw additional horizontal lines in Figure 8 showing the slope inferred for the Local Group, RXJ1340.6+4018 and Centaurus A and SDSS galaxy clusters (the middle two are so close that they are hard to resolve). The SDSS

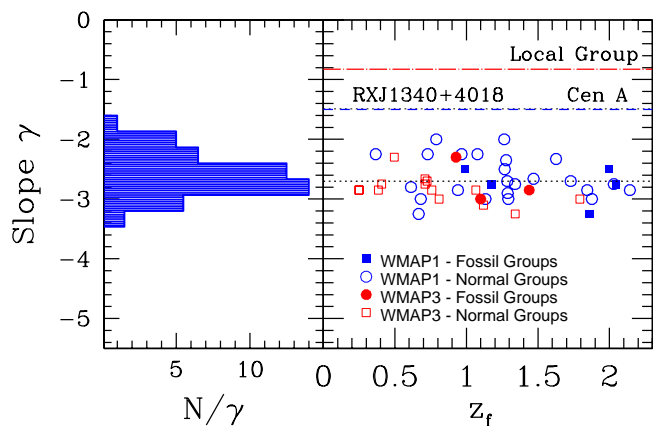


**Figure 8.** *Left Panel.* The slope distribution of all the group sized halos of the samples. *Right Panel.* Slopes of the subhalo function versus formation redshift for all the halos in the two simulations (WMAP1/WMAP3). The slopes inferred for the observed SDSS galaxy cluster sample, the Local Group, Centaurus A and RXJ1340.6+4018 are also indicated for comparison.

galaxy cluster slope quoted by Desai et al. (2004) is  $\gamma = -2.614 \pm 0.042$  in fair agreement with numerical simulations. This shallower value quoted for SDSS data is because it is estimated over the entire range of  $V_{circ}/V_{par}$ , whereas the slope of the simulations is obtained in a narrower range (for  $0.1 < V_{circ}/V_{par} < 0.3$ ). However, the observed slopes of galaxy groups like Centaurus A and RXJ1340.6+4018 are substantially lower.

## 4 SUMMARY

RXJ1340.6+4018 has a typical mass of 25% of the Virgo cluster mass, but it exhibits a substructure population similar to the rescaled version of the Local Group. We used numerical simulations of group sized halos to examine the formation of systems with paucity of substructures like the fossil system RXJ1340.6+4018.

Our results show that:

- In the mass range  $1-5 \times 10^{13} M_{\odot}$  almost 18% of the group sized halos are candidate fossil groups according to the definition of velocity gap, but not a single system has a shallow cumulative substructure function similar to that one exhibited from the Local Group or RXJ1340.6+4018.

- Current observations of galaxy groups with a velocity gap exhibit a paucity of substructures with a substructure function like that of the Local Group, whereas the total number of substructures predicted from CDM models is almost constant and independent of any gap in velocity.

- The total number of substructures identified at the present time does indeed correlate with the formation time of the halo, as found in semi-analytics work. However, the early formation time reduces the average number of substructures by a factor two, while a factor of six is needed to reconcile the predictions with the observations. We showed that only the normalization of the cumulative velocity function of satellites depends on the formation time, whereas the slope does not. This seems intuitive as the fluctuations

in CDM models are gaussian with random phases. While the early formation of a parent halo from a large scale wave will bias the formation of substructures, it should not and indeed does not tilt the smaller scale spectrum.

- We find that the cumulative velocity distribution function of substructures is self-similar in CDM models, with the slope being the same in the WMAP1 and WMAP3 realizations and they agree with previous results on halos with galaxy masses and galaxy clusters. Yet, only the slope of the cumulative velocity function of substructures in the SDSS galaxy cluster sample agrees with the predictions of the numerical simulations, while the slopes of groups of galaxies like the Local Group, Centaurus A or the RXJ1340.6+4018 are significantly shallower.

We explored the effects of cosmic variance on the cumulative substructure function and find that the deviation of the model predictions from the observations begins for subhalos with circular velocity larger than a 20% of the parent halo circular velocity. For a typical galaxy group sized halo with circular velocity of  $450 \text{ km s}^{-1}$ , a missing subhalo in the observations has a circular velocity of  $\sim 80 \text{ km s}^{-1}$ .

Physical mechanisms invoking reionization or feedback processes from satellites are already stretching to suppress halos at  $30 \text{ km s}^{-1}$ . Here we showed that invoking an earlier formation time for these objects may alleviate the problem but cannot reproduce the observed number of visible galaxies in groups of galaxies with intermediate mass between galaxies and poor cluster of galaxies.

If future spectroscopic luminosity function for X-ray emitting groups in the range of mass intermediate between the Local group and the Virgo cluster produces a larger sample of groups with paucity of substructures this class of objects will remain an interesting challenge for the current model of structure formation.

## ACKNOWLEDGMENTS

The numerical simulations were performed on zBox2 supercomputer at the University of Zurich; (<http://www-theorie.physik.unizh.ch/~dpotter/zbox2/>).

E.D. thanks highlighting discussions with Daniele Pierini, Maurizio Pannella and Stefano Zibetti on observational data. E.D. is financed by a EU Marie Curie Intra-European Fellowship under contract MEIF-041569.

## REFERENCES

- Benson, A. J., Frenk, C. S., Lacey, C. G., Baugh, C. M., & Cole, S. 2002, MNRAS, 333, 177
- Bertschinger, E. 2001, ApJS, 137, 1
- Bullock J. S., Kravtsov A. V., Weinberg D. H., 2000, ApJ, 539, 517
- Cypriano, E.S., Mendes de Oliveira, C.L., Sodre', L. Jr. 2006, AJ, 132, 514
- De Lucia, G., Kauffmann, G., Springel, V., White, S. D. M., Lanzoni, B., Stoehr, F., Tormen, G., Yoshida, N. 2004, MNRAS, 348, 333
- Desai, V., Dalcanton, J. J., Mayer, L., Reed, D., Quinn, T., Governato, F., 2004, MNRAS, 351, 265
- Diemand, J., Kuhlen, M. & Madau, P. 2007, ApJ submitted, (astro-ph/0703337)

- D’Onghia, E., & Lake, G. 2004, *ApJ*, 612, 628
- D’Onghia, E., Sommer-Larsen, J., Romeo, A. D., Burkert, A., Pedersen, K., Portinari, L., & Rasmussen, J. 2005, *ApJL*, 630, L109
- Faber, S.M., Jackson, R.E. 1976, *ApJ*, 204, 668
- Gastaldello, F. et al. 2007, *ApJ*, in press, (astro-ph/0703461)
- Hernquist, L., Katz, N., Weinberg, D. H. 1995, *ApJ*, 442, 57
- Jones, L. R., Ponman, T. J., Forbes, D. A. 2000, *MNRAS*, 312, 139
- Jones, L.R., Ponman, T.J., Horton, A., Babul, A., Ebeling, H., Burke, D.J. 2003, *MNRAS*, 343, 627
- Katz, N., White, S.D.M. 1993, *ApJ*, 412, 455
- Kazantzidis, S., Mayer, L., Mastropietro, C., Diemand, J., Stadel, J., & Moore, B. 2004, *ApJ*, 608, 663
- Kleyna, J. T., Wilkinson, M. I., Evans, N. W., & Gilmore, G. 2005, *ApJL*, 630, L141
- Klypin, A., Kravtsov, A., Valenzuela, O., Prada, F. 1999, *ApJ*, 522, 82
- Klypin, A., Macciò, A. V., Mainini, R., & Bonometto, S. A. 2003, *ApJ*, 599, 31
- Kravtsov, A. V., Gnedin, O. Y., & Klypin, A. A. 2004, *ApJ*, 609, 482
- Mainini, R., Macciò, A. V., Bonometto, S. A., & Klypin, A. 2003, *ApJ*, 599, 24
- Macciò, A., Moore, B., Stadel, J., Diemand, J. 2006a, *MNRAS*, 366, 1529
- Macciò, A. V., Moore, B., Stadel, J., & Potter, D. 2006b, proceedings of the XLIst Rencontres de Moriond, astro-ph/0609146
- Macciò, A., Dutton, A., van den Bosch, F., Potter, D., Stadel, J. 2007, *MNRAS* in press (astro-ph/0608157)
- Mateo, M. L. 1998, *ARA&A*, 36, 435
- Mayer, L., Kazantzidis, S., Mastropietro, C., Wadsley, J. 2007, *Nature*, 445, 738
- Miles, T. A., Raychaudhury, S., Forbes, D. A., Goudfrooij, P., Ponman, T. J., & Kozhurina-Platais, V. 2004, *MNRAS*, 355, 785
- Moore et al. 1999, *ApJL*, 524, L19
- Odenkirchen, M., et al. 2001, *AJ*, 122, 2538
- Ponman, T.J. et al. 1994, *Nature*, 369, 462
- Somerville, R. S. 2002, *ApJL*, 572, L23
- Spergel, D. N., et al. 2003, *ApJS*, 148, 175
- Spergel, D. N., et al. 2006, (astro-ph/0603449)
- Stadel, J. G. 2001, Ph.D. Thesis, University of Washington
- Strigari, L., Bullock, J., Kaplinghat, M., Diemand, J., Kuhlen, M., Madau, P. 2007, *ApJ* submitted (astro-ph/0704.1817)
- van den Bosch, F. C., et al. 2007, *MNRAS*, 139
- Vikhlinin, B.R. et al. 1999, *ApJ*, 520, L1
- Wechsler, R. H., Bullock, J. S., Primack, J. R., Kravtsov, A. V., & Dekel, A. 2002, *ApJ*, 568, 52
- Willman, B. et al. 2005, *ApJ*, 626, L85
- Zentner, A. R., Berlind, A. A., Bullock, J. S., Kravtsov, A. V., & Wechsler, R. H. 2005, *ApJ*, 624, 505